Available online at www.sciencedirect.com
SCIENCE DIRECT
Applied Catalysis B: Environmental 60 (2005) 233–243
APPLIED CATALYSIS B: ENVIRONMENTAL
www.elsevier.com/locate/apcatb

In situ visible microscopic study of molten $Cs_2SO_4{\cdot}V_2O_5$–soot system: Physical interaction, oxidation rate, and data evaluation

Agus Setiabudi, Niels K. Allaart, Michiel Makkee *, Jacob A. Moulijn

Section Reactor and Catalysis Engineering, Faculty of Applied Sciences, Delft University of Technology, Julianalaan 136, NL 2628 BL Delft, The Netherlands

Received 6 October 2004; received in revised form 15 March 2005; accepted 21 March 2005
Available online 27 April 2005

Abstract

In situ visible microscopy has been used to characterise the physical interaction between soot and $Cs_2SO_4{\cdot}V_2O_5$, a potentially attractive catalyst, under oxidation conditions. Upon heating to its melting point, $Cs_2SO_4{\cdot}V_2O_5$ shows both mobility and attachment to the soot particle. This creates a liquid catalyst–soot–gas interface that is favourable for the oxidation reaction. Microscope image data can be used to estimate the oxidation rate, which is in good agreement with data obtained from TGA and fixed bed experiments.

Keywords: $Cs_2SO_4{\cdot}V_2O_5$; Liquid catalyst; Diesel soot oxidation; Contact soot catalyst

1. Introduction

For the catalytic reaction between a solid reactant and a gaseous reactant in the presence of a solid catalyst, contact between the catalyst and the solid reactant is a key factor to initiate reaction that takes place at the solid reactant–solid catalyst–gas interface. Catalysed diesel soot oxidation is a good example of this. Earlier, it was demonstrated that when soot was mixed with the metal oxide catalyst in a ball mill (''tight contact''), the oxidation rate is much higher than when soot and the catalyst was mixed by spatula (''loose contact'') [1]. It has been shown that under practical conditions in a catalytic filter loose contact rather than tight contact is encountered. Therefore, a soot–catalyst mixture prepared for example by ball mill mixing is not representative for practical application.

To solve the problem, the catalyst–soot contact should be created in situ without exerting mechanical forces. A completely different route is the following. So-called mobile catalysts can establish mobility either via volatilisation or surface migration. They enable an intense interaction between reactants and catalyst. In the oxidation of soot with Cu/K/V/Cl or Cu/K/Mo/Cl catalysts, the presence of volatile compounds dispersed over the soot particle has been concluded to produce activity [2,3]. Another class of catalysts that are capable to create a catalyst–soot contact are molten salt catalyst, for example, $Cs_2SO_4{\cdot}V_2O_5$, $CsVO_3{\cdot}MoO_3$, and $Cs_2O{\cdot}V_2O_5$ of which surface migration is thought to create the catalyst mobility [4–6]. These catalysts show high activities at and above their melting points, i.e. 625, 635, and 655 K, respectively. The mobility of the catalyst particle and the wetting of carbon surface have been acknowledged to increase the catalyst activity in the oxidation of carbonaceous material due to a better catalyst–carbonaceous contact [7,8].

Molten salts diesel soot oxidation can have some drawback in some practical application. These drawbacks can be related to either thermal degradation or selective leaching in condensed water in the soot oxidation process (one of the components of the molten salt is partially evaporated or dissolved, respectively).

Although catalyst–soot contact has been generally acknowledged as a very important factor for the catalytic soot oxidation with mobile catalyst, the chemical mechanism and the physical interaction between catalysts and soot

* Corresponding author. Tel.: +31 15 2781391; fax: +31 15 2785006.
E-mail address: m.makkee@tnw.tudelft.nl (M. Makkee).

0926-3373/$ – see front matter © 2005 Elsevier B.V. All rights reserved.
doi:10.1016/j.apcatb.2005.03.005

remain unclear. Based on different experimental methods, several hypotheses on the physical interaction of soot particle with mobile catalyst were proposed. In an ex situ SEM study of a partly burnt soot/catalyst ($Cs_2SO_4{\cdot}V_2O_5$) sample, it was shown that the soot particles were sheltered inside the salt [4]. This observation suggests that a liquid catalyst can establish a tight interaction with the soot particle leading to a covering of the soot particle. However, such an ex situ study is not a direct proof. Further clarification had been done by means of in situ SEM [5]. In that study soot was partly dispersed on $Cs_2SO_4{\cdot}V_2O_5$ deposited on alumina crucible at 5 mbar oxygen atmospheres. By this method, catalyst mobility was observed but soot wetting, however, could not be demonstrated.

To have a better understanding on the molten salt–catalyst–soot contact, an in situ study with realistic oxidation conditions, temperature and oxygen partial pressure, is needed. In this study, an in situ visible microscopy has been used to characterise the physical interaction between the soot and the mobile catalyst during the oxidation process. Attempt to use the microscope observation images to estimate the oxidation rate is also discussed. Emphasis is put on the potential and limitation of this experimental method.

2. Experimental

2.1. Materials

$Cs_2SO_4{\cdot}V_2O_5$, a molten salt catalyst, was used. The catalyst was prepared based on the methods described by Jelles et al. [4]. Cs_2SO_4 and V_2O_5 were mixed in a 55–45 molar ratio as was reported in literature [9] to yield an eutectic mixture with a melting point of 625 K. The components were mixed in a mortar and put in a ceramic cup. This ceramic cup was placed in an oven and heated up to 725 K at 5 K/min, which is 100 K above the expected melting point, and kept there for 2 h. The sample was cooled down to room temperature at 10 K/min. Subsequently, the catalyst was crushed in a mortar and sieved in a size fraction smaller than 100 μm. In addition to molten salt, vanadium (V) oxide and caesium sulfate (both from Aldrich) were used to represent immobile catalyst. The soot material used is Printex-U, a flame soot from Degussa.

2.2. Microscope observation

The microscope experiments were performed with a Leica DMLM microscope with a long distance objective of 50 times magnification (PL Fluotar L50x/0.55). The image generated by the microscope was recorded by YC 05 II camera and transferred to a computer. A sample was placed on a 7 mm diameter stainless steel disc and placed in a high temperature Linkam TS1500 in situ cell sample holder as presented in Fig. 1. The onset figure outlined the inside assembly of the cell. Over the sample, air was flown at 100 ml/min flow rate. A temperature controller Linkam TMS 93 was used to carry out temperature programmed experiments. Image observations were done both at the increase of temperature and at isothermal conditions. For the temperature programmed experiments the heating rate was 5 K/min.

2.3. TGA experiment

A TGA experiment with a ‘controlled’ catalyst–soot wetting area was performed. A soot layer was placed into a 6 mm diameter alumina crucible and gently pressed in order to create a soot layer with a bowl-like surface. The soot layer mass was 5.2 mg. A catalyst grain (about 4.2 mg) was placed on the centre of the bowl-like surface of the soot layer. The mixture was heated to 625 K at 5 K/min in flowing He. It

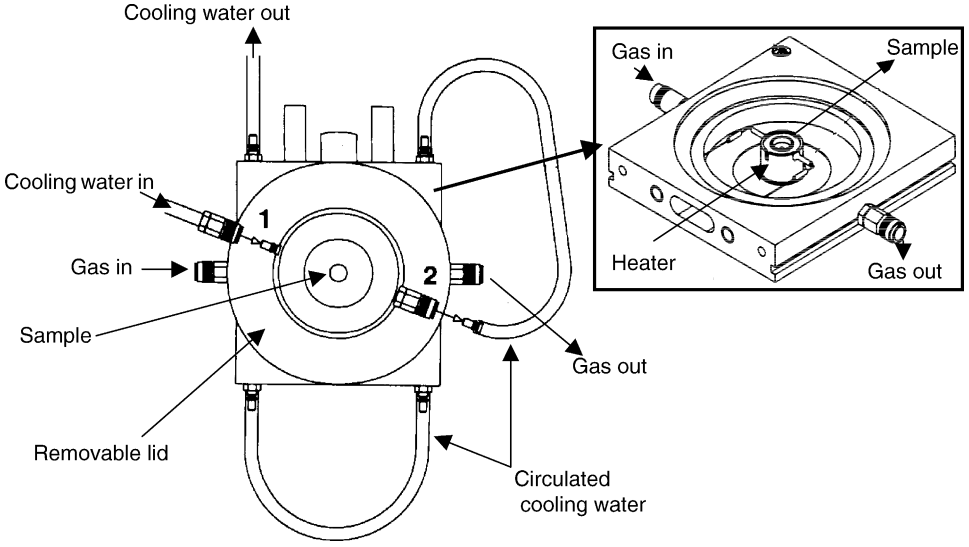

Fig. 1. Schematic figure of in situ reactor cell for the microscope observation.

was expected that the catalyst would either spread over the surface of soot layer or burn a hole in the soot layer. At 625 K the gas flow was switched to 100 ml/min air and kept there for 4 h. The oxidation rate at 625 K was determined and used as a comparison for the soot oxidation rate determined using microscopic data.

3. Image analysis; estimation of soot cluster size and oxidation rate

The image analysis methods used by Samson et al. [10] to evaluate the fractal dimension of soot agglomerate based on TEM observation was adapted to analyse the microscope image obtained in this study. The procedure was followed to determine the projected image area of the soot particle. The microscope images, originally in colour, were converted to a grey scale mode and viewed as electronic grid of 512 × 512 pixels. Each pixel is viewed as a grey level that can have a value of 0–255. The grey level of 0 signifies the darkest grey, while the 255 is the lightest grey level. An appropriate grey level threshold, between 140 and 160, was chosen to distinguish the soot image from the catalyst image. For example if the threshold is chosen to be 150, all pixels from 150 to 255 are reset to white, while pixels with grey level from 0 to 150 are reset to black. The manual threshold was applied until the shape of the evaluated soot image was congruent with the corresponding original image. A MATLAB program calculates the ratio of pixels occupied by soot image to the total pixels when all images are set to white. This ratio is proportional with soot image area relative to the total image.

The projected area of soot is used to predict the number of soot primary particles (n_{pp}). There are several methods to estimate the number of primary particle in a soot aggregate, normally by assuming that soot aggregates have a fractal-like structure. Generally, the relation between the number of primary particle and the radius of gyration (R_g) of an aggregate, as shown in Eq. (1), can be used [11]

$$n_{pp} = k_f \left(\frac{R_g}{d_{pp}}\right)^{D_f} \quad (1)$$

where d_{pp} represents diameter of primary particle, k_f represents a constant fractal pre-factor, and D_f represents the fractal dimension of the agglomerate.

Another method is to use the relation between the number of primary particles and the projected area of aggregate/cluster. In the investigation of fractal properties of soot, Köylü et al. [12] performed TEM observations on soot aggregate generated from a variety of fuels (ethyne, propene, ethene, and propane). They found a relationship between the projected image area of cluster and the number of primary particle as presented in Eq. (2)

$$n_{pp} = 1.15 \left(\frac{A_{cl}}{A_{pp}}\right)^{1.09} \quad (2)$$

where A_{cl} is the projected area of cluster; obtained from microscope image analysis and A_{pp} the projected area of primary particle.

In this study relationship expressed in Eq. (2) is used since the cluster area can be directly obtained from the microscope image analysis. Therefore, n_{pp} can be directly determined. Assuming that the primary particle diameter, d_{pp}, is 20 nm and that the density of primary particle of graphite is 2150 kg/m^2, the number of primary particle and the mass of soot cluster could be calculated. Based on the soot mass of the observed cluster and time needed for the soot image to disappear completely, the oxidation rate was determined. The statistic reliability of the calculated rate is still a matter of debate. The soot oxidation experiments have been repeated three times in time and with different operators and the observed phenomena were identical. In each oxidation experiment three or four soot–catalyst interactions have been followed in time and each interactions have been analysed and interpreted. Since the main objective of this paper is the verification that the contact between molten salts and soot and how this contact is maintained for the complete conversion the statistic reliability is less important.

4. Results

4.1. Visible physical process upon heating and melting of catalyst and catalyst–soot mixture

A series of microscope images recorded when $Cs_2SO_4{\cdot}V_2O_5$ catalyst was heated in the in situ cell on a metal plate of a sample holder are shown in Fig. 2. Three catalyst particles were initially observed. Their sizes were ca. 30–50 μm and they had a bright yellow colour at room temperature. Upon heating, the colour of the catalysts transformed to red-brown at 535 K (Fig. 2b) and at the same time the shape of the catalyst particles was slowly transformed. At 545 K, the two neighbouring particles that had a distance of about 5–10 μm started moving and agglomerated to form a bigger particle, see Fig. 2c. This process is ascribed as catalyst agglomeration.

Upon heating to higher temperature, the colour remained unchanged. At 585 K (Fig. 2d), the catalyst particle that still had irregular edges expanded and at 600 K, the expanded solid collapsed (Fig. 2e). As the temperature was kept constant for 3 min the catalyst particle spread and formed a viscous droplet (Fig. 2f). Raising the temperature to 625 K caused spreading of the droplet (Fig. 2g and h). At this temperature most part of the catalyst melted. When the heated catalyst was cooled down it crystallised, and the colour turned back to original bright yellow at 535 K (Fig. 2i). At room temperature a more crystallite appearance is observed and more catalyst spreading was observed over the metal disc (Fig. 2j). In other words, a re-dispersion of the large catalyst particles to smaller particles has taken place.

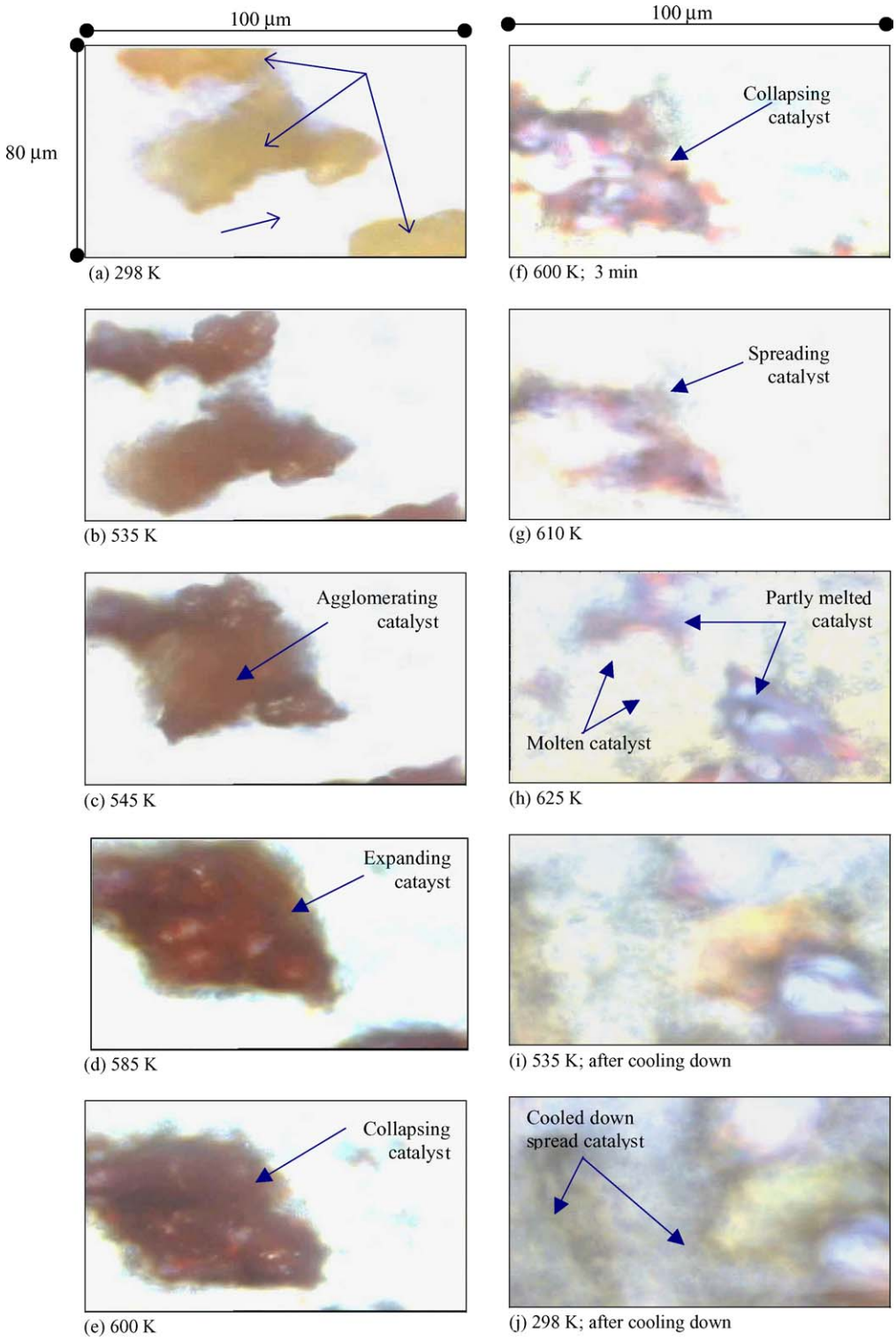

Fig. 2. Microscope images of $Cs_2SO_4{\cdot}V_2O_5$ catalyst particle heated at 5 K/min in 100 ml/min flowing air. The images were taken at 50× magnification.

When a mixture of catalyst and soot was heated from room temperature to 625 K, the images are presented in Fig. 3. Two $Cs_2SO_4{\cdot}V_2O_5$ catalyst grains of ca. 30–60 µm touch a soot particle, assigned as soot 1, of ca. 30 µm particle size (Fig. 3a). The colour transformation as observed in the pure catalyst can be seen at 473 K (Fig. 3b). Around 535 K, some of the catalyst edges were moving (Fig. 3c) and at 555 K the catalyst expanded (Fig. 3d). At the same time the soot particle was moving, while it remained attached to the same edge of the catalyst.

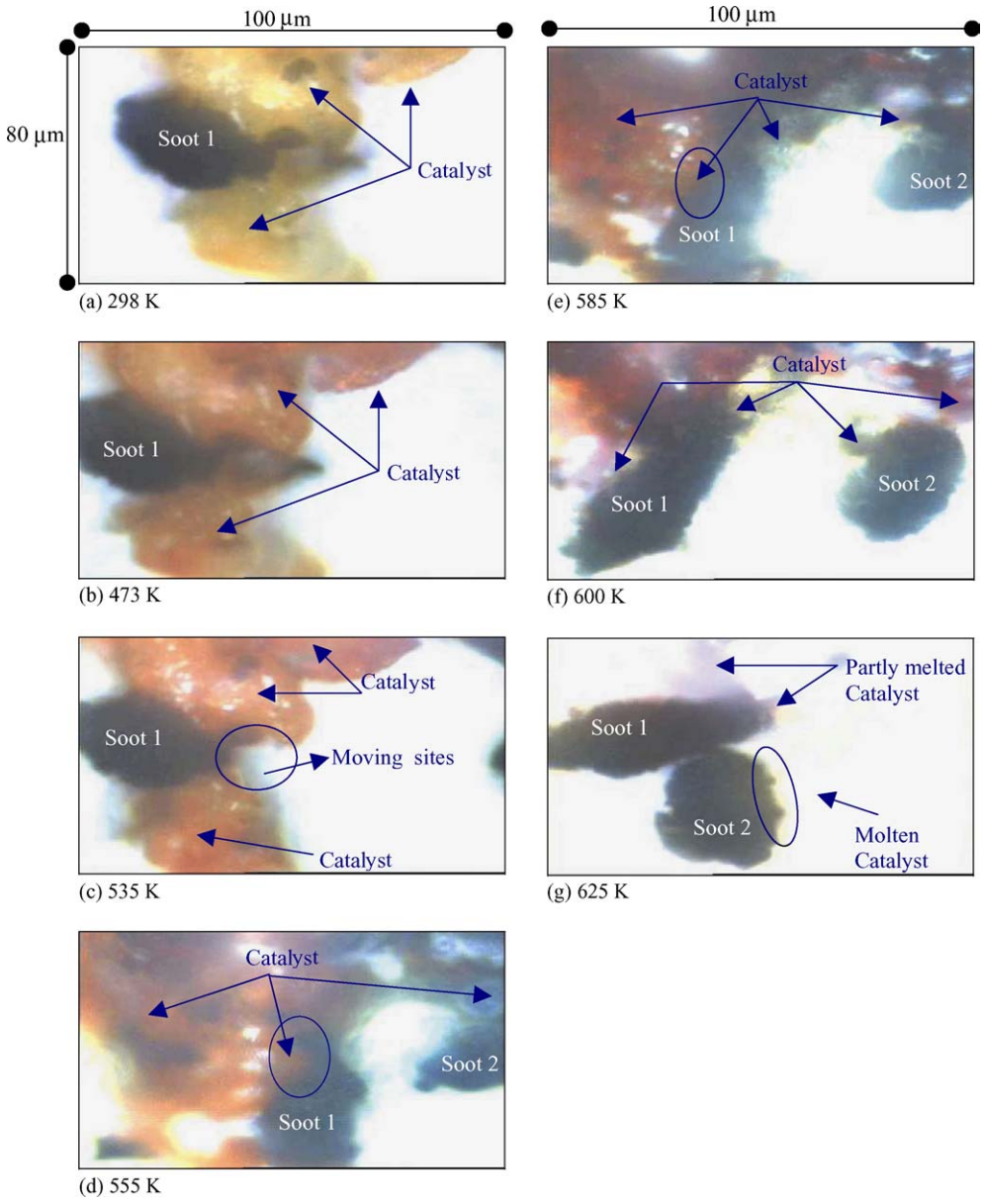

Fig. 3. Microscope images of $Cs_2SO_4{\cdot}V_2O_5$ catalyst–soot mixture heated at 5 K/min in 100 ml/min flowing air taken at several temperatures. Soots 1 and 2 represent two different soot particles. The images were taken at 50× magnification.

Indication of catalyst spreading over the soot particle was observed and marked by the circle (Fig. 3d and e). Furthermore, at 555 K a new soot particle appeared in the view and was assigned as soot 2.

From 555 to 585 K, the edges between the catalyst and the soot became unclear (Fig. 3d and e). Between 585 and 600 K the catalyst expanded gradually as indicated by the movement of soot position attached to the catalyst (Fig. 3e and f). At 600 K, the catalyst collapsed and smaller particles were observed (Fig. 3f). The edges between the catalyst and soot became blurred and the soot particles moved over the catalyst film formed over the sample holder. At 625 K, most of the catalyst particle spread almost evenly over the sample holder reflecting a white-bright colour, and simultaneously, the soot particle moved on top of the catalyst layer. A small part of the catalyst remained solid and is assigned as partly melted catalyst (Fig. 3g).

At 625 K, the catalytic soot oxidation progress was followed as a function of time. The images are shown in Fig. 4. A partly melted catalyst particle and two soot particles, soots 1 and 2, were initially observed (Fig. 4a). Part of the soot 1 edge was intimately attached to the partly melted catalyst while most part of the soot was on top of the molten catalyst. In 2 min, the soot 2 orientation was changed. Surrounding the soot particle, a tiny yellow image could be observed as marked by the circle in Fig. 4a–c. Both soot particles continued to shrink (Fig. 4c and d), and disappeared after about 14 min.

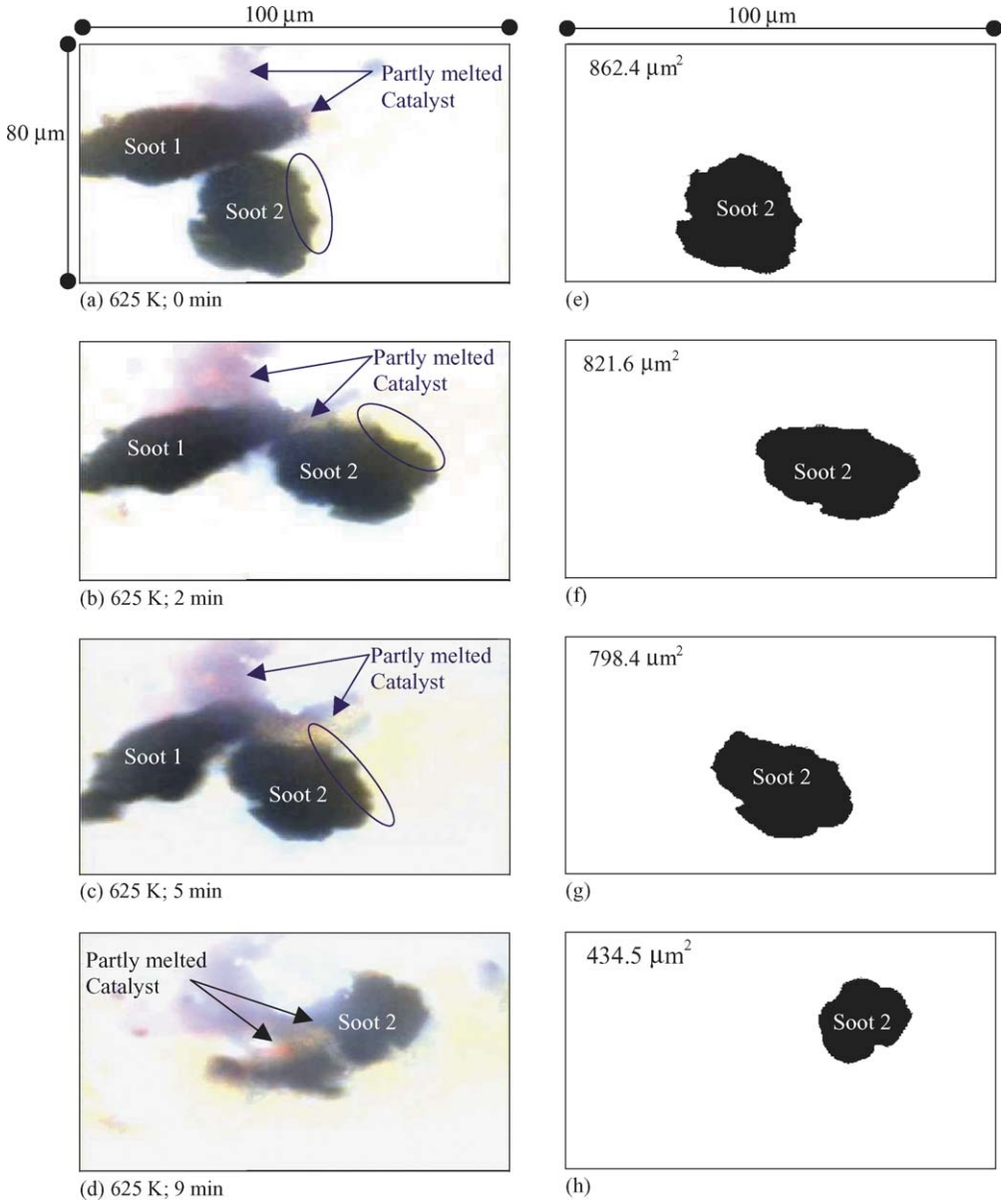

Fig. 4. (a–d) Demonstration of the $Cs_2SO_4{\cdot}V_2O_5$ catalytic effect at 625 K; in situ microscope observation of $Cs_2SO_4{\cdot}V_2O_5$ catalyst–soot mixture in 100 ml/min flowing air taken as a function of time. Soots 1 and 2 represent two different soot particles. The images were taken at 50× magnification. (e–h) Examples of image area calculation results and the projected area of the images.

Fig. 4e–h shows examples of soot 2 images that have been analysed by the method described in Section 3. The projected areas of analysed corresponding soot images are also incorporated. It is clearly shown that at 625 K the projected areas of soot 2 decreased as a function of time.

When V_2O_5 or Cs_2SO_4 was used to replace the $Cs_2SO_4{\cdot}V_2O_5$, no soot attachment by the catalyst, neither soot movement, nor soot shrinkage could be observed. These observations only for V_2O_5 are presented in Fig. 5. Upon heating to 625 K no movement of the soot and the V_2O_5 or Cs_2SO was observed. When the mixture was kept at 625 K for 90 min both soot and catalyst sizes remained unchanged. Only a colour transformation of V_2O_5 was observed at 525 K.

4.2. Estimation of oxidation rate

The projected area determination procedure was done for the microscope images observed at 625, 645, and 665 K. The results are presented in a plot. This plot correlates the fraction of remaining image area as a function of time on stream, as can be seen in Fig. 6. The oxidation rate increases with the increase of temperature. At 625 K a rather flat curve is observed at the first 5 min, suggesting that the soot areas decrease very slowly. Latter on a sharp curve is observed suggesting that the soot area decreases very fast. Throughout this paper this sharp curve is referred to as ‘fast decrease period’. At 645 K a similar curve is produced, except that the

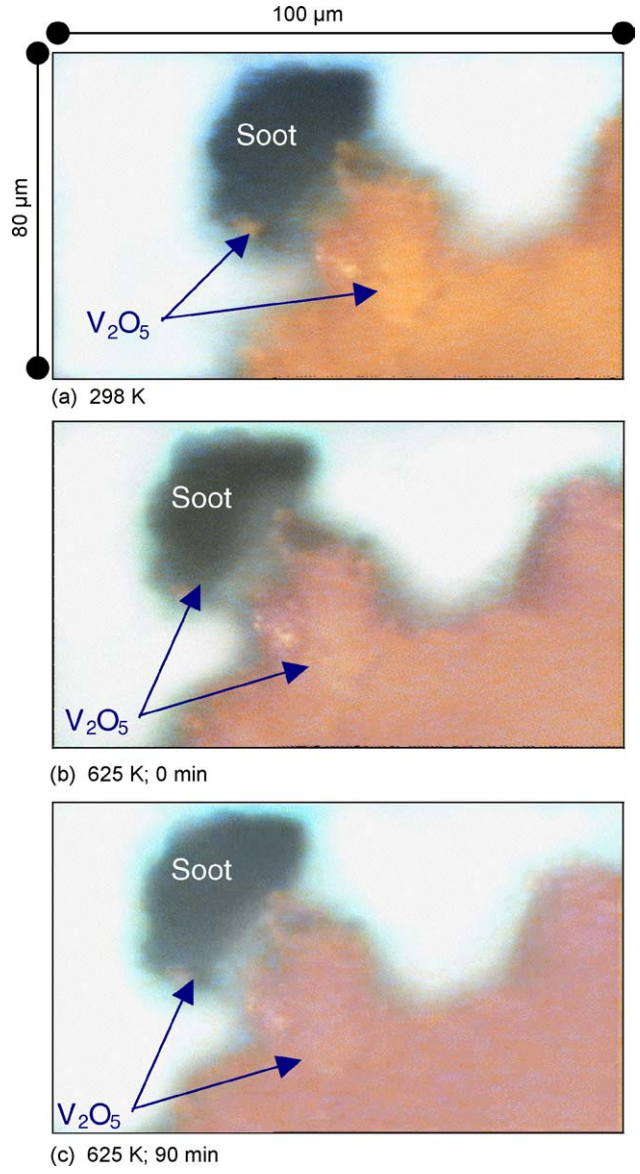

Fig. 5. Microscope images of V_2O_5 catalyst–soot mixture heated at 5 K/min in 100 ml/min flowing air. The soot and the catalyst are steady at their position. The images were taken at 50× magnification.

time corresponding for the flat curve is shorter. At 665 K only a fast decrease of soot area is observed.

Based on the procedure described in Section 3, the overall oxidation rates were calculated. The data are summarised in Table 1. The oxidation rates of the fast decrease period were also calculated. For comparison the average oxidation rate obtained from TGA and flow reactor experiments are also incorporated. The oxidation rate measured in TGA experiment is based on 1.4×10^7 μm^2 contact area. This contact area was obtained by assuming that the catalyst particle spread over the bowl-like soot layer, and the spreading area was assumed to be 50% of the crucible cross-sectional area. In flow reactor experiment, 20 mg soot was mixed with 40 mg catalyst in loose contact procedure using 10% O_2.

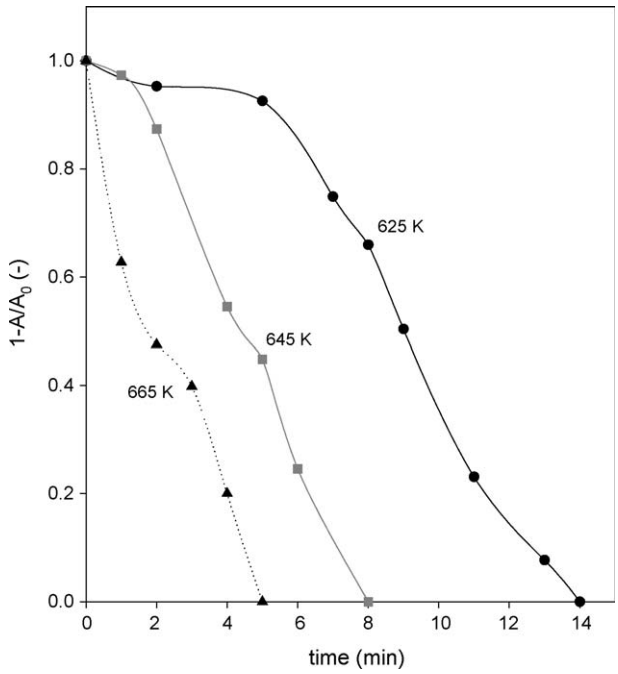

Fig. 6. Fraction of remaining soot as a function of time at different constant temperatures estimated from the microscope image area.

To have a fair comparison, the oxidation rates are normalised to the estimated initial contact area. It is shown that the normalised oxidation rates obtained from microscopic study and TGA experiment are in the same order of magnitude. This is also the case when the oxidation rate was compared to that of the flow experiment.

The activation energy of $Cs_2SO_4{\cdot}V_2O_5$ catalysed soot oxidation was calculated from overall oxidation rate data and the fast decrease period. The overall activation energy was found to be 88.4 kJ/mol, while the activation energy of the fast decrease period is 51.6 kJ/mol. It should be noted for both soot oxidation and catalytic soot oxidation an activation energy of 150 kJ/mol is reported [4,5].

5. Discussion

5.1. Physical interaction

Upon heating to 625 K, the molten salt catalyst ($Cs_2SO_4{\cdot}V_2O_5$) and V_2O_5 or Cs_2SO_4 showed a different behaviour with respect to their mobility. Particle movement and agglomeration are characteristic for the heated ‘‘molten salt’’ catalyst, particularly between 535 and 600 K. In contrast to $Cs_2SO_4{\cdot}V_2O_5$, V_2O_5 was immobile both when the temperature programmed was applied and when it was kept at 625 K for 90 min. It has to be noted that the melting point of V_2O_5 and Cs_2SO are 963 and 1283 K, respectively. When soot was mixed with ‘‘molten salt’’ catalyst the soot particles were intimately attached to the moving catalyst. Furthermore, catalyst spreading over the soot particle was

Table 1
Summary of calculation data in the determination of oxidation rate based on microscope image

Temperature (K)	Initial projected image area[a], A_0 (μm^2)	Number of primary particles, n_{pp}	Soot mass (μg)	Time needed to complete the oxidation (s)	Oxidation rate ($\mu g/s$)		Normalised oxidation rate ($\mu g/s\ m^2$)	
					Overall	Fast decrease period	Overall	Fast decrease period
Microscope observation								
625	862	1.20×10^7	1.08×10^{-4}	840	1.30×10^{-7}	1.83×10^{-7}	1.50×10^{-4}	2.10×10^{-4}
645	835	1.16×10^7	1.04×10^{-4}	480	2.17×10^{-7}	2.38×10^{-7}	2.59×10^{-4}	2.85×10^{-4}
665	803	1.10×10^7	0.99×10^{-4}	300	3.33×10^{-7}	3.33×10^{-7}	4.14×10^{-4}	4.14×10^{-4}
TGA experiment								
625	1.40×10^{7}[b]				5.8×10^{-3}		4.14×10^{-4}	
Flow reactor experiment								
625	13.3×10^{7}[c]				6.0×10^{-2}		4.51×10^{-4}	

[a] Calculated using image analysis methods described in Section 3 and assumed as catalyst–soot wetting area.
[b] Estimated wetting area in TGA experiment; 50% of TGA crucible cross sectional area.
[c] Estimated from catalyst mass ratio to experiment in TGA (40 mg in flow reactor experiment 4.2 mg in TGA experiment).

observed. No clear indication of liquid spreading over the soot particle was observed when the catalyst melted at 625 K. Only a tiny yellow image surrounding the soot particle appeared during the first 5 min.

On the one hand these observations clearly demonstrated the mobility characteristics of the two types of materials up to 625 K. On the other hand, upon heating both $Cs_2SO_4{\cdot}V_2O_5$ and V_2O_5 showed the similar colour transformation that can be related to the formation of reduced V_2O_5 in the mixture. The formation of VO_2, V_2O_3, V_2O_4 or V_6O_{13} is, among others, not surprising and can explain the change in colour. VO_2 and V_2O_3 for example have a black colour [13], and might cause the red-brown colour, due to mixing with the yellow colour, as observed above 475 K.

It remains unclear if the tiny yellow image surrounding the soot particle, Fig. 5a–c, can be attributed to the molten catalyst, wetting the soot particle. The soot movement over the catalyst layer, however, indicated that the soot particle was on top of the liquid catalyst. It is most likely that the soot particle is partly dipped into the liquid catalyst. In this situation a liquid catalyst–soot–oxygen interface is created, which is favourable for the oxidation reaction to take place. Another situation that might occur is that the soot particle is fully dipped/covered by the catalyst film. In this circumstance, oxygen transport from the gas bulk through the catalyst film to the liquid catalyst–soot interface is required. It is expected that in catalyst melting point regime, the partly dipped soot situation will occur, as the soot density is relatively low in comparison with the molten salt. These two liquid catalyst–soot contact situations together with the assumed reaction mechanism are presented in Fig. 7.

In situ microscope observation at 625 K provides excellent data to visually demonstrate the catalytic effect of molten $Cs_2SO_4{\cdot}V_2O_5$ in the oxidation of soot. As can be compared from Figs. 4 and 5, the presence of V_2O_5 or Cs_2SO_4 does not lead to the reduction of soot size even when it was kept for 90 min. On the contrary, it needs only 14 min to oxidise a relatively larger soot particle with $Cs_2SO_4{\cdot}V_2O_5$ catalyst. These facts raise the question on the active component in $Cs_2SO_4{\cdot}V_2O_5$ catalyst. If V_2O_5 or Cs_2SO_4 would be the active component in the molten salt, the question is how the liquid state facilitates V_2O_5 to become active.

At first sight it might seem conflicting to assume that V_2O_5 is the active component in $Cs_2SO_4{\cdot}V_2O_5$ catalyst, since V_2O_5 alone has been shown in this study to be inactive. It has, however, to be noted that V_2O_5–soot mixture was prepared by the loose contact procedure. Furthermore, it has been reported that V_2O_5–soot mixture prepared in tight contact procedure showed a much lower combustion temperature than that of V_2O_5–soot mixture prepared in loose contact [1]. In the study with in situ high-temperature XRD, V_2O_5 in tight contact with charcoals in air was reduced to V_6O_{13} at 575–675 K [14]. So, if the active component in molten $Cs_2SO_4{\cdot}V_2O_5$ catalyst is V_2O_5, it can be postulated that in molten $Cs_2SO_4{\cdot}V_2O_5$ the soot particle should also be in tight contact with V_2O_5.

It is worthwhile to briefly review the difference between the solid and the liquid state with respect to particle and molecular mobility. In solid phase the 'molecule' is rigid and highly ordered. In the liquid (molten) state it is less ordered, has high kinetic energy, and is very mobile. These properties allow 'the dissolved V_2O_5 species' in molten $Cs_2SO_4{\cdot}V_2O_5$ catalyst to freely move, and when the soot particle is dipped into the molten $Cs_2SO_4{\cdot}V_2O_5$, this mobile V_2O_5 has a chance to disperse over the soot particle and make contact at a more ''molecular level''. At this stage oxidation of soot by V_2O_5 via oxygen transfer mechanism might take place. Conversely, V_2O_5 'molecule' in solid V_2O_5 is rigidly attached in the solid state and is immobile; as a result it is difficult to make contact with soot at 'molecular level'. This hypothesis is illustrated in Fig. 8.

The processes following the microscope observation upon heating of $Cs_2SO_4{\cdot}V_2O_5$, $Cs_2SO_4{\cdot}V_2O_5$–soot, and V_2O_5–soot can be outlined as follows. A contact between the

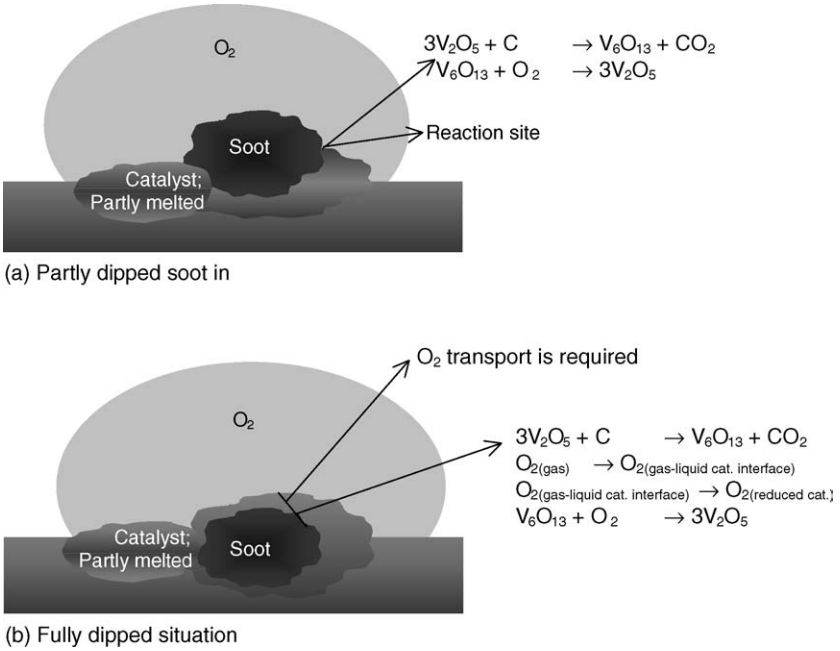

Fig. 7. Impression of possible catalyst–soot wetting situation and its possible effect to the kinetics molten salt catalysed soot oxidation.

soot particle and the $Cs_2SO_4{\cdot}V_2O_5$ can be established before the catalyst melted. This was shown by soot attachment to the moving catalyst while indication of catalyst spreading over the soot particle is observed. When the catalyst was in its liquid state, the soot particle is partly dipped into the liquid leading to the creation of a very intimidate catalyst–soot–oxygen interaction, at which it is favourable for the soot oxidation to take place. On the contrary no such behaviour was observed for the V_2O_5–soot mixture.

5.2. Interpretation of microscope data to estimate oxidation rate

Originally, the plot of soot fraction as a function of time was directly used to estimate the trend of oxidation rate as a function of time. The two-dimensional imaging can, however, disturb the quantitative interpretation of the microscope data. In Fig. 6, the type of curve observed at 625 K showed two different regimes, viz. the flat curve during the first 5 min of observation and a sharp decrease period curve for the rest of the time. The flat curve could be explained by very slow soot shrinkage. However, since the curve was derived from two-dimensional images, another explanation based on a possible artefact of the technique might be valid.

Fig. 9 describes how two-dimensional microscope data may lead to a misinterpretation. In the microscope observation of partly dipped soot, the arrangements from bottom to top are the liquid catalysts, the soot, and the observer. At situation t_1, the catalyst–soot contact is located at the downside of the soot particle. For soot with sphere-like shape, the image taken from the topside is recorded as two-

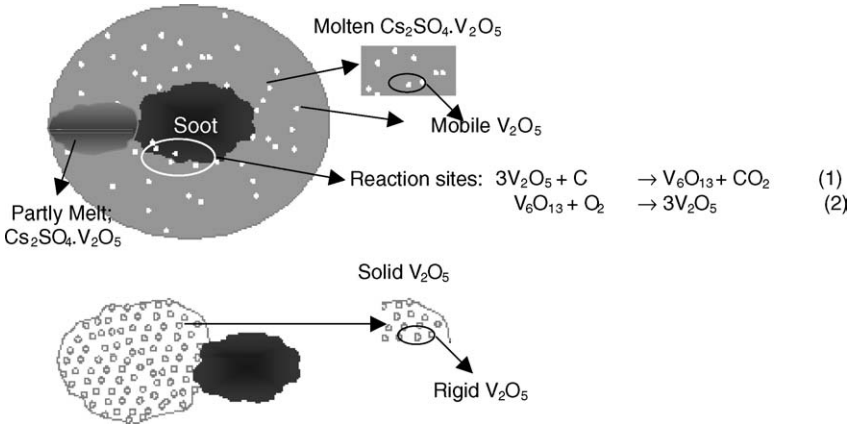

Fig. 8. Illustration of soot–catalyst interactions in molten $Cs_2SO_4{\cdot}V_2O_5$–soot mixture and solid V_2O_5–soot mixture; top view interpretation. Note that reduced form of vanadium oxide can also be VO_2 and V_2O_3.

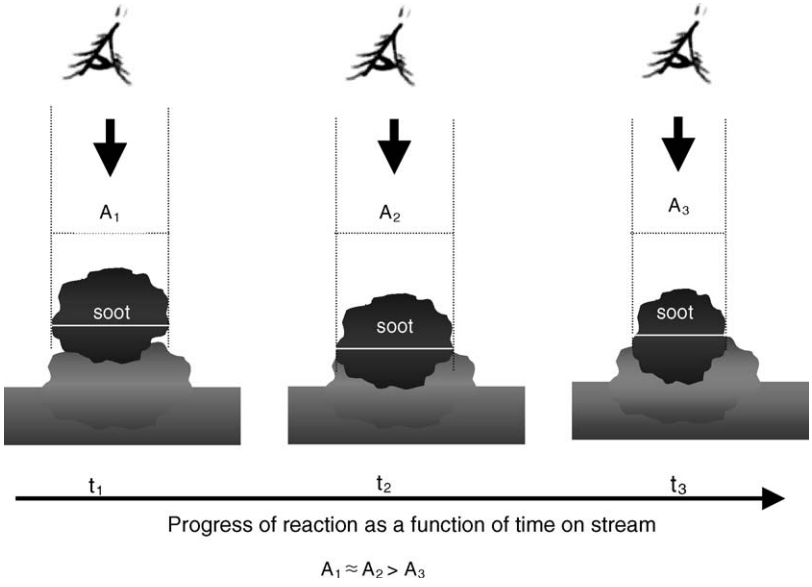

Fig. 9. Possible catalyst–soot contact situation that might lead to misinterpretation of microscope observations.

dimensional images and simplified to a circle. When oxidation occurs, it takes place at the liquid catalyst–soot contact site and although soot combustion takes place, the recorded image area does not decrease significantly. As a result, the images at t_1 and t_2 would be essentially identical. A reduction of image area only starts when the catalyst–soot contact reaches the diameter of the sphere, t_2. The plot is useful to demonstrate relative oxidation rates at different temperatures. As can be seen, the soot image disappears very fast when the oxidation takes place at high temperature.

The calculation of normalised oxidation rates was based on the assumption that the contact area in microscope observation is the same as the projected image area, and in TGA experiment that it is about 50% of crucible cross-sectional area. It is clear that the normalised oxidation rate estimated by means of microscope data is in the same order of magnitude with that of obtained from TGA experiment. It is possible that the estimation of contact area in TGA experiment is too low, for example if soot capillary wetting by the molten catalyst would be considered the predicted wetting area would be higher and as a result, the predicted oxidation rate will be much closer. Based on visual observation of soot–catalyst spot before and after TGA experiment, the destruction of soot layer via molten salt catalysed soot oxidation can be illustrated by a series of processes as shown in Fig. 10. These results showed the importance of contact area between molten catalyst and the soot particle. It is shown that the oxidation rate is proportional to the liquid catalyst–soot wetting area.

For the sake of comparison, the oxidation rate data was further compared to that of the flow reactor oxidation rate. Although it is difficult to estimate the wetting area of soot by the catalyst in that experiment, it is obvious that the amount of catalyst used is much higher than in TGA experiment (40 mg in flow reactor compared to 4.2 mg in TGA experiment). As a result, the soot wetting area in the flow reactor experiment is also higher leading to much higher oxidation rates than in TGA experiment. However, the normalised oxidation rate is, once again, in the same order of magnitude with that of predicted from the microscope observation.

The difference between the activation energy obtained from overall oxidation rates and from the fast decrease period is reported in Table 1. The calculated activation energy are significantly lower than the reported activation energies for both soot as catalytic soot oxidation of 150 kJ/

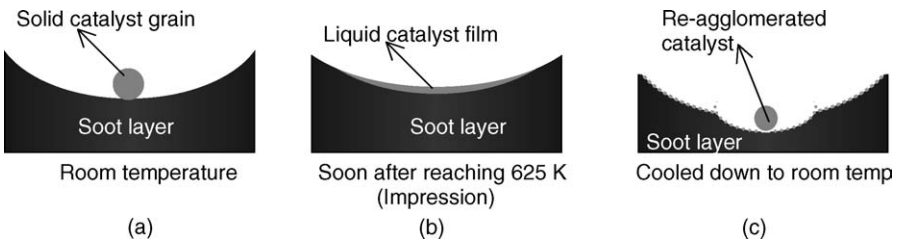

Fig. 10. Interpretation of catalyst–soot contact during TGA experiment; (a) solid catalyst–soot at room temperature, (b) catalyst spreading over the soot layer at catalyst liquid state temperature regime, (c) cooled down catalyst–soot mixture of incomplete TGA experiment.

mol [4,5]. The calculated oxidation rate in the microscope will be probably caused by mass transport limitations. The observed rates in the microscope are, however, in agreement with the observed rates in the TGA and fixed-bed reactor. Also the oxidation rate started when the molten salt catalyst is transferred in from the solid phase into the liquid phase. The observed temperature, when the soot oxidation is started is in agreement with the reported and observed melting point of the eutectic mixture. It is beyond the scope of this paper to judge the accuracy of activation energy obtained.

The interpretation of microscope data to estimate oxidation rate can be summarised as follows. The trend of decreasing image area should be interpreted carefully as this not always reflects the actual decrease of soot mass. By assuming that soot has a fractal like structure, the soot mass can be predicted from its cluster image area from which the overall oxidation rate can be determined. When the rate is compared to that obtained from TGA and a conventional fixed bed reactor, nice agreement is observed. Furthermore, this study gives a clear picture on the influence of catalyst wetting on the oxidation rate.

6. Conclusions

1. In situ visible microscopy gives valuable data on wetting characteristics of molten salt catalysed oxidation of soot. The rate data obtained agree well with those measured in TGA and fixed bed reactors, but at low conversions an artefact of the microscopic technique can lead to a serious underestimation of the rate of reaction.
2. Upon heating to its melting point, $Cs_2SO_4{\cdot}V_2O_5$ catalyst shows both mobility and attachment on soot particle.
3. In a catalyst liquid state, soot particle can be (partly) dipped into the liquid catalyst leading to a liquid catalyst–soot–oxygen interface that is favourable for the oxidation to take place.
4. Catalytic effect of molten salt catalyst is clearly demonstrated at 625 K shown by the much faster soot shrinkage in molten catalyst–soot mixture compared to that of metal oxide–soot.
5. The microscope image data should be interpreted very carefully, especially when the soot shrinkage is followed as a function of time.

References

[1] J.P.A. Neeft, M. Makkee, J.A. Moulijn, Chem. Eng. J. 64 (1996) 29.
[2] Y. Watabe, C. Yamada, K. Irako, Y. Murakami, European Patent EP0092023.
[3] Ciambelli, V. Palma, S. Vaccaro, Catal. Today 17 (1993) 71.
[4] S.J. Jelles, B.A.A.L. van Setten, M. Makkee, J.A. Moulijn, Appl. Catal. B 21 (1999) 35.
[5] B.A.A.L. van Setten, R. van Dijk, S.J. Jelles, M. Makkee, J.A. Moulijn, Appl. Catal. B 21 (1999) 51.
[6] D. Fino, N. Russo, C. Badini, G. Saraco, V. Specchia, AIChE J. 49 (8) (2003) 2173.
[7] D.W. McKee, C.L. Spiro, P.G. Kosky, E.L. Lamby, Fuel 64 (1985) 805.
[8] D.W. McKee, Carbon 8 (1970) 623.
[9] Gmelins Handbuch der Anorganische Chemie V B2 (1967) 492.
[10] R.J. Samson, G.W. Mulholand, J.W. Gentry, Langmuir 3 (1987) 272.
[11] R. Julien, R. Botet, Aggregation and Fractal Aggregates, World Scientific Publishing Co., Singapore, 1987.
[12] Ü.Ö. Köylü, G.M. Faeth, T.L. Farias, M.G. Carvalho, Combust. Flame 100 (1995) 621.
[13] http://4.1911encyclopedia.org/V/VA/VANBRUGH.htm.
[14] I.F. Silva, C. Palma, K. Kimkiewicz, S. Eser, Carbon 36 (7/8) (1998) 861.